Carbohydrate Polymers 113 (2014) 430–437

Contents lists available at ScienceDirect

Carbohydrate Polymers

journal homepage: www.elsevier.com/locate/carbpol

Preparation and swelling behavior of a novel self-assembled β-cyclodextrin/acrylic acid/sodium alginate hydrogel

Zhanhua Huang[a,b,*], Shouxin Liu[a], Bin Zhang[a], Qinglin Wu[b]

[a] Key Laboratory of Bio-based Material Science and Technology of the Ministry of Education, Northeast Forestry University, Harbin 150040, China
[b] School of Renewable Natural Resources, Louisiana State University Agricultural Center, Baton Rouge, LA 70803, USA

ARTICLE INFO

Article history:
Received 8 January 2014
Received in revised form 6 July 2014
Accepted 7 July 2014
Available online 14 July 2014

Keywords:
β-Cyclodextrin
Hydrogel
Biodegradable
Retention properties
Salt resistance

ABSTRACT

A novel biodegradable β-cyclodextrin/acrylic acid/sodium alginate (CSA) hydrogel with a three-dimensional network structure was self-assembled by inverse suspension copolymerization. The CSA resin was pH sensitive and had good water absorption properties in pH 6–8 buffer solutions. At a β-CD:AA:SA mass ratio of 1:9:3 the CSA water absorbency was found to be 1403 g/g and the CSA hydrogel strength was 4.968 N. In 0.005–0.1 mol/L chloride salt and sulfate salt solutions the CSA water absorbencies increased as follows: $NaCl > KCl > MgCl_2 > CaCl_2 > FeCl_3$, and $Na_2SO_4 > K_2SO_4 > FeSO_4 > Al_2(SO_4)_3$, respectively. The release of water from the CSA hydrogel occurred slowly over 120 h. The biodegradation efficiency of the resin reached 85.3% for *Lentinula edodes*. The super water absorbency, good salt resistance and excellent water retention properties of CSA make it suitable for application as an agricultural water retention agent in saline soils.

1. Introduction

Superabsorbent polymers (SAPs) have recently been developed as functional materials and they can absorb up to thousands of times their own weight in water in addition to having excellent water retention properties. Because of their strong affinity with water, SAPs are widely used in personal hygiene products, medical materials, preservation materials, civil engineering materials, and environmental improvement materials (Blanco-Fernandez, Lopez-Viota, Concheiro, & Alvarez-Lorenzo, 2011; Li, Kim, & Lee, 2009; Yang, Xie, & He, 2011). Because of the increased demand for scarce water resources, SAPs have important roles in areas such as agriculture, forestry, landscaping, and desert improvement (Achtenhagen & Kreuzi, 2011; Huang, Liu, Fang, & Zhang, 2013b). They have a broad potential market.

SAPs can be divided into three categories: starch-grafted, cellulose-grafted and synthetic resins, and these depend on the source. For the first two categories, starch or cellulose is the substrate, respectively, and these are grafted and copolymerized with hydrophilic vinyl or vinyl monomers and possess post-hydrolysis hydrophilicity (Kabiri, Omidian, Zohuriaan-Mehr, & Doroudiani, 2011). Most industrially produced SAPs are synthetic resins and high water absorption properties are easily achieved. However, acrylic superabsorbent resins are not easily biodegraded and are harmful to human health and, therefore, these are not environmentally friendly materials. SAPs produced by starch-grafted copolymerization have high water absorption and water retention rates but poor salt resistance (Zou et al., 2012). Cellulose-grafted SAPs are cheap and have high gel strengths, few soluble ingredients, strong anti-enzymatic abilities, and are biodegradable (Bao, Ma, & Li, 2011). As a result they have gradually attracted attention and are expected to become the most active area of superabsorbent research and development.

β-Cyclodextrin (β-CD) is a cyclic oligosaccharide formed by seven glucose molecules through α-1,4-glucoside bonds. It contains the same chemical structural unit (glucose molecules) as cellulose. The most significant feature of β-CD is that it has outer-ring hydrophilic, inner-ring hydrophobic as well as size-defined three-dimensional microenvironmental chiral cavities. Its molecules have a tapered cylindrical shape, which enables them to accommodate other hydrophobic molecules or groups of suitable sizes in the cavities to produce inclusion complexes (Misiuk & Zalewska, 2009). β-CD can be used in applications such as drug delivery (Yallapu, Jaggi, & Chauhan, 2010), environmental protection (Shao, Sheng, Chen, Wang, & Nagatsu, 2010), and as gene markers (Srinivasachari & Reineke, 2009). β-CD is biodegradable and has a wide variety of sources. Several hydroxyl groups with the same chemical reactivity are distributed over the

* Corresponding author at: Key Laboratory of Bio-based Material Science and Technology of the Ministry of Education, Northeast Forestry University, Harbin 150040, China. Tel.: +86 451 82192905; fax: +86 451 82192905.
E-mail address: huangzh1975@163.com (Z. Huang).

http://dx.doi.org/10.1016/j.carbpol.2014.07.009
0144-8617/

molecular surfaces and etherification, oxidation, substitution, and graft polymerization reactions can be carried out using these hydroxyl groups (Badruddoza, Tay, Tan, Hidajat, & Uddin, 2011; Huang, Liu, Zhang, Xu, & Hu, 2012; Murthy, Madhav, Kumar, Rao, & Nageswar, 2009; Zhang, Qin, He, Li, & Zhang, 2009). The chemical structure and physical properties of β-CD suggest that it could replace cellulose synthetic SAPs. However, for the use of β-CD in the synthesis of SAPs it is necessary to increase its molecular weight by attaching monomers. β-CD molecules intended for SAPs can be used as a skeleton for graft polymerization and their polyhydroxy structure can give products with three-dimensional network structures. Additionally, complexes can be formed with metal ions and included organic materials, and product biodegradability can be improved. The superabsorbent materials will, therefore, have more features. However, with the exhaustion of petroleum resources, it has become the global attention focus in producing fuel and chemicals from renewable biomass resource. Acrylic acid (AA) as a kind of petrochemical product material in the SAPs, the price showed a trend of rising year by year in recent years, and the price from $2600 per ton in 2010 rose to $4560 per ton in 2011 (Lv, 2011) and keep rising in 2013. How to use some renewable products to substitution of acrylic acid in SAPs on the premise of not reduce product water absorption performance, this is the purpose of adding sodium alginate. Sodium alginate is a natural polysaccharide compounds, come from natural marine resources such as kelp, seaweed and so on. The price of industrial grade sodium alginate was about $4500 per ton in 2013, the price was stable in recently years. Sodium alginate is biodegradable and has lots —OH groups and —COONa (H) groups. Those groups will increase the pH application ranges of product. It would be worthwhile and a very meaningful thing that if sodium alginate can be used to replace part of AA in the absorbent resin, reducing the amount of petroleum products AA, at the same time, the water absorption performance of absorbent resin not be decreased, and due to the addition of SA can also make resin with the characteristics of biodegradable.

In this study, β-CD, acrylic acid (AA), and sodium alginate (SA) were used as raw materials. An inversion suspension method was used to produce a biodegradable β-CD based superabsorbent (CSA) material with a three-dimensional network structure by graft copolymerization. The effect of crosslinking agent, initiator, neutralization, reaction time, reaction temperature, and CSA raw material ratio on water absorbency was investigated. The chemical structure, micromorphology and water absorption as well as the release properties of CSA in salt solutions are discussed.

2. Experimental

2.1. Materials

β-Cyclodextrin (β-CD), acrylic acid (AA), sodium alginate (SA, M_w = 105,000, η = 2.19), *N*,*N*′-methylenebisacrylamide (NMBA), ammonium persulfate (APS), and all sulfate and chloride salts were purchased from the Chemical Reagent Development Center of Kemiou Engineering (Tianjin, China). All reagents used were of analytical grade and all solutions were prepared using distilled water.

2.2. Preparation of CSA

A weighed quantity of β-CD and NaOH (1 mol/L) solution were put into a 250 mL four-necked flask equipped with a stirrer. Nitrogen was flowed through the flask for 10 min and the reaction temperature was increased to 60–65 °C. SA, AA and NMBA at certain mass ratios were then added. After 15 min, certain quantities of initiator (APS) and crosslinking agent (NMBA) were added using a funnel at a constant rate of 1–2 d/s with stirring. The mixture was allowed to react for 2–3 h under nitrogen. The mixture was filtered, washed several times with ethanol and distilled water and dried at 50 °C for 48 h to a constant weight. A range of CSA products were obtained by changing the reaction conditions such as the mass ratios of β-CD, AA, and SA, the dosages of APS and NMBA, the reaction time, and the neutralization degree. The optimal reaction conditions were thus determined. CSA resin was firstly washed at room temperature with ethanol for 4–6 h to remove unreacted monomer and initiator and after at 90 °C with the same solvent for 8 h in a closed stainless steel vessel to remove poly(AA) homopolymer. Then the treated CSA was dried under vacuum at 40 °C overnight and weighed. Such procedure was repeated until constant weight of the sample was obtained. At this point it was assumed that unreacted species and poly(AA) homopolymer were completely removed. The amount of grafted poly(AA) homopolymer (Barsbay & Güven, 2013), termed degree of grafting (DG) was calculated as follows:

$$DG(\%) = \frac{W - W_0}{W_0} \times 100 \quad (1)$$

where W_0 is the weight of virgin CSA resin and *W is* the weight of the grafted CSA resin after above washing procedure, respectively.

2.3. Characterization

Scanning electron microscopy (SEM) images were obtained using a FEI QUANTA 200 microscope (FEI Corporation, Hillsboro, OR, USA). Fourier-transform infrared (FTIR) spectroscopy was performed with a MAGNA 560 FTIR spectrometer (Thermo Nicolet Corporation, Waltham, MA, USA) using KBr disks from 4000 cm^{-1} to 500 cm^{-1}. Solid-state ^{13}C cross-polarization magnetic-angle spinning nuclear magnetic resonance (^{13}C CPMAS NMR) spectra of β-CD and CSA were obtained using a Bruker Avance 400 FT-NMR spectrometer (Bruker Optics Inc., Billerica, MA, USA), at a frequency of 75.47 MHz with sample spinning at 4.0 kHz. The impulse duration at 90° was 4.2 ms and the contact time was 1 ms. The number of transients was about 1000 and the decoupling field was 59.5 kHz. Chemical shifts were determined relative to tetramethylsilane.

2.4. Water absorbency of CSA in different solutions

Chloride and sulfate solutions were prepared at different concentrations (0.1, 0.05, 0.01, 0.005 mol/L) and 0.05 g of CSA was added to 100 mL of each salt solution. The water absorbency was measured. CSA (0.5 g) was added to 100 mL of pH 2, 4, 6, 8, 10, and 12 buffer solutions. After saturation, the CSA hydrogels were filtered and weighed and the absorbency *Q* was calculated as follows:

$$Q = \frac{m - m_0}{m_0} \quad (2)$$

where m_0 is the mass of CSA and *m is* the mass of the CSA hydrogel sample.

2.5. CSA gel strength

CSA hydrogels of 1 cm × 1 cm in size were weighed and labeled as models for the tests. The pressure at which the hydrogel was crushed was determined using a HY-0230 small material testing machine (Shanghai Yiheng Corporation, China) at a test rate of 1.0 mm/min.

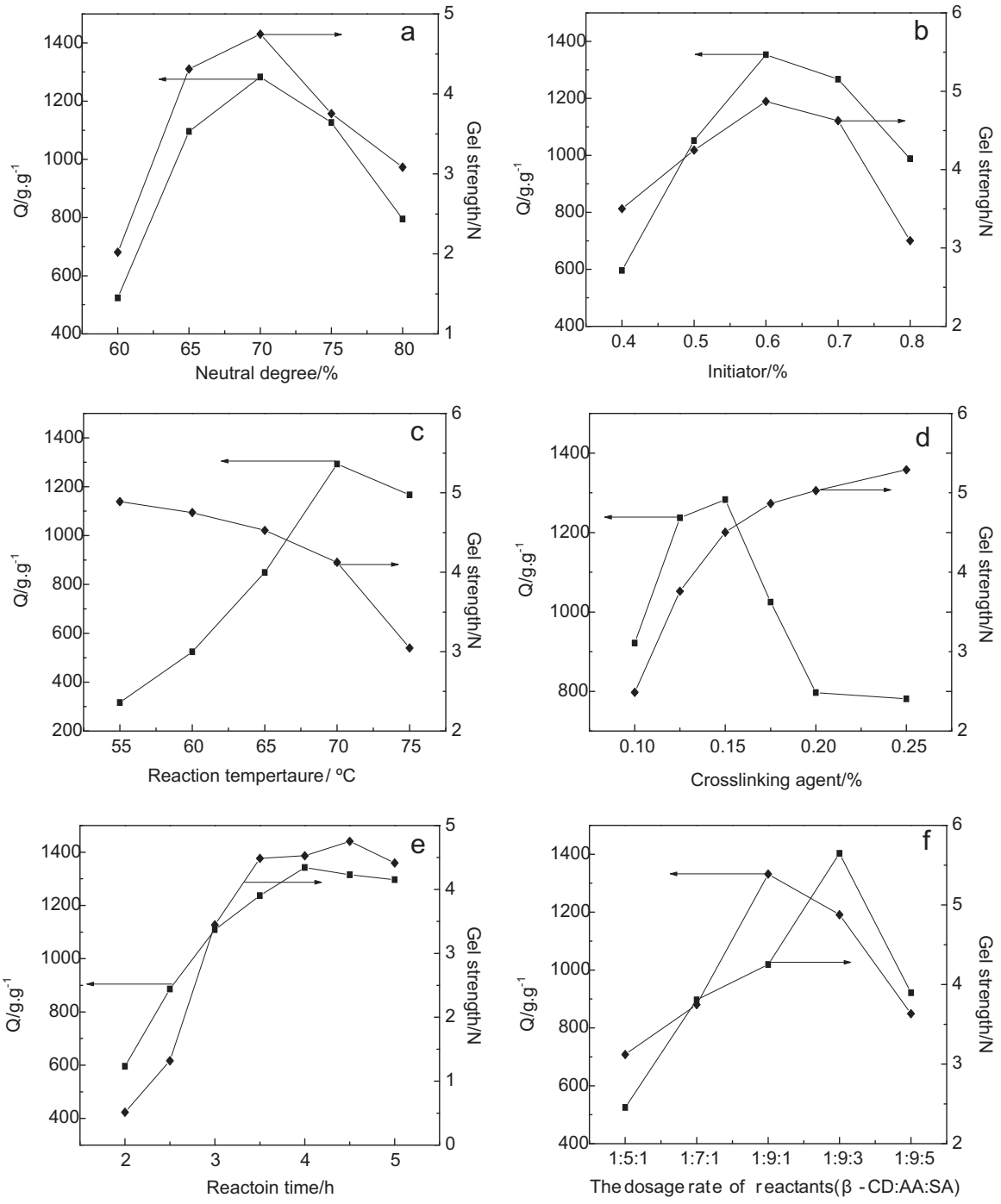

Fig. 1. Effect of experimental conditions for CSA on its water absorbency and gel strength.

3. Results and discussion

3.1. CSA preparation for the best swelling properties

The effects of neutralization degree on the water absorption capacity and gel strength are shown in Fig. 1(a). Fig. 1(a) shows that with an increase in neutralization degree the water absorbency of the product first increases and then decreases. The water absorbency and gel strength were both highest when the neutralization degree of AA was 70%. When the neutralization degree was relatively low, a large amount of —COOH groups were present and the molecular chain conformation between the crosslinking points was curly, which was not conducive to water swelling. The AA reactivity was relatively high and the polymerization reaction was difficult to control when the neutralization degree of AA was low. A highly crosslinked homopolymer formed easily resulting in a resin with a relatively low water absorption capacity and gel strength (Pourjava & Amini-Fazl, 2007). When the neutralization degree was greater than 70%, the excess H^+ influenced the generation of free radicals in the system because the reaction between β-CD radicals and monomers is nucleophilic, and this affected the graft copolymerization. In another system, the number of —COOH groups was too small and the number of hydrogen bonds between polysaccharide chains and carboxyl groups was thus inadequate.

Because the crosslinking density was too low and the resin-based three-dimensional network structure was limited the CSA water absorbency and gel strength was very low.

The effects of initiator concentration on the CSA water absorption capacity and gel strength are shown in Fig. 1(b). As the initiator concentration increased, both the water absorbency and gel strength of the product first increased and then decreased. When the amount of initiator used was 0.6% of the total monomer mass, the maximum distilled water absorbency of CSA was 1353 g/g and the gel strength was 4.85 N. The amount of initiator determined the number of active centers in the system and affected the reaction rate. This was a very important experimental factor. When the amount of initiator was less than 0.6% the water absorbency of the resin increased with an increasing amount of initiator. At more than 0.6% the water absorbency decreased with an increase in the amount of initiator. If the amount of initiator is not sufficient, only a small number of free radicals are formed and the number of reactive sites in the reaction system will be limited, preventing the resin from forming an effective three-dimensional crosslinked structure. With a large amount of initiator, the number of generated free radicals will be high and the crosslinking reaction will occur rapidly. The formed resin will thus have a highly branched three-dimensional tight structure, which does not swell easily in water. All the molecular chains in the three-dimensional network structure were short and as a result the gel strength was low (Ma et al., 2011).

The effect of reaction temperature on the water absorbency and gel strength of CSA is shown in Fig. 1(c). From Fig. 1(c) the absorbance of distilled water by CSA increased and then decreased with an increase in reaction temperature, and it reached a maximum at 70 °C. However, the CSA gel strength gradually decreased with an increase in reaction temperature. The reasons for this are that with an increase in reaction temperature, the polymerization rate also increases and the half-life of the initiator becomes shorter. The number of free radicals formed per unit time thus increases, chain transfer and chain termination are facilitated, and the average relative molecular weight of the product decreases. The branched chains between the crosslinked structures of the final product become shorter and the arrangement between the main chains is more irregular while the crosslinking density decreases or becomes uneven. Thus, during water absorption the polymer chain cannot swell sufficiently to absorb more water and the resulting gel is softer and of lower strength.

Fig. 1(d) shows the effect of crosslinking agent on the water absorbency of CSA and gel strength. As shown in Fig. 1(d), the absorbency first increased and then decreased with an increase in crosslinker mass, and the absorbency was maximum when the mass of crosslinking agent was 0.15% that of the monomer. The CSA gel strength increased with an increase in the amount of crosslinking agent. In this study, the main role of the crosslinking agent is to promote a certain degree of crosslinking of the macromolecular chains of the β-CD, AA, and SA copolymer to enable the polymer to form a network structure with large three-dimensional spaces for water absorption. As the amount of crosslinker increases the number of crosslinking points in the reaction system gradually increases and the absorbency and gel strength of the product increase accordingly (Peng, Xu, Peng, Wang, & Zheng, 2008). In the presence of excess crosslinker the crosslinking point density within the polymer is too large and a dense grid structure is formed. The product gel strength increased but the product grid structure expanded with difficulty after water swelling. Therefore, the water absorbency of CSA decreased. Based on the absorbency and gel strength of CSA the appropriate amount of crosslinker was 0.15% of the total monomer mass.

The effects of reaction time on the CSA water absorbency and gel strength are shown in Fig. 1(e). With an increase in the reaction time, both the water absorbency and gel strength first increased and then decreased slightly. The water absorbency was highest when the reaction time was 4 h. In this study, the reaction time had a significant impact on the resin's absorbency. The polymerization reaction was incomplete when the reaction time was too short and the product had a relatively low molecular weight. Few product swelling and expansion spaces were present and the resin absorbency was low. When the reaction time exceeded 4 h, the polymerization reaction achieved steady-state polymerization with equal radical formation and disappearance rates and this constitutes a dynamic balance, i.e., the length of the reaction period had no influence. However, when the reaction time was too long the stirring of the reaction system resulted in a shearing environment over a long period and this shearing force damaged the resin-based three-dimensional network structure and, therefore the CSA water absorbency and gel strength were slightly reduced (Xu, Li, & Sun, 2010). Experiments showed that 4 h was the optimum reaction time.

Fig. 1(f) shows the effect of the raw material mass ratios on the CSA water absorbency and gel strength. In this study, β-CD acted as a crosslinked network backbone and the amount of β-CD had to be limited. When the β-CD:AA:SA mass ratio was 1:5:1, 1:7:1, 1:9:1, 1:9:3, 1:9:5, the grafting degree of AA was 72.6%, 76.7%, 79.3%, 78.1%, and 69.5%, respectively. Moreover, when the β-CD:AA:SA mass ratio was 1:9:3, the CSA water absorbency was maximum, i.e., 1403 g/g, and the CSA hydrogel strength was relatively high (4.968 N). When the amount of AA was low, not enough monomer or β-CD was present for grafting and crosslinking with SA. Thus, the CSA had an imperfect network structure with a low crosslinking degree and low water absorbency in addition to low gel intensity. Increasing the amount of AA improved the crosslinking degree of CSA, increased the number of hydrophilic groups and enhanced the water absorbency property of CSA. However, too much AA increased the probability of homopolymerization during crosslinking, which led to the crosslinking degree and the density of CSA increasing, and the water absorbency of CSA decreasing. SA was added to reduce the amount of AA to ensure a sufficient number of hydrophilic carboxyl groups in CSA without decreasing its water absorption abilities. The addition of β-CD and SA also increased the biodegradability of the product. With the increase of the dosage of SA, the grafting degree of AA and the CSA water absorbency were decreased. As a result, the best β-CD:AA:SA mass ratio was found to be 1:9:3.

3.2. Structural characterization of CSA

3.2.1. FTIR spectra

Fig. 2 shows the IR spectra of β-CD and CSA. The IR spectrum of β-CD has peaks at 3410 cm^{-1} from the stretching vibrations of —OH, 2930 cm^{-1} from the asymmetric stretching vibrations of —CH, 1640 cm^{-1} from the asymmetric stretching vibrations of C—O and C—H, 1160 cm^{-1} from the stretching vibrations of —C—O—C, 1070 cm^{-1} from the bending vibrations of —C—O—H, and 1030 cm^{-1} from the coupling vibrations of C—O and C—C (Huang et al., 2013b). In the IR spectrum of the product, the original and strong —OH peak of β-CD at 3410 cm^{-1} became weaker, and a broad peak of medium or low intensity appeared at 3430 cm^{-1}, indicating that the introduction of a raw material with two —OH stretching vibrations and with different intensities increased the number of —OH forms present. This causes the —OH peak to shift and widen. This result indicated that some β-CD had already been polymerized with AA. The characteristic β-CD absorption peaks at 2930, 1070, and 1030 cm^{-1} from C—H, C—O, and C—C, respectively, were retained. A broad —C=O stretching vibration peak appeared at 1700 cm^{-1}, and it masked the β-CD absorption peak at 1640 cm^{-1}. Two types of —C=O vibration peaks were present in CSA and the overlap of these peaks at 1700 cm^{-1} resulted in a broad peak. These two —C=O

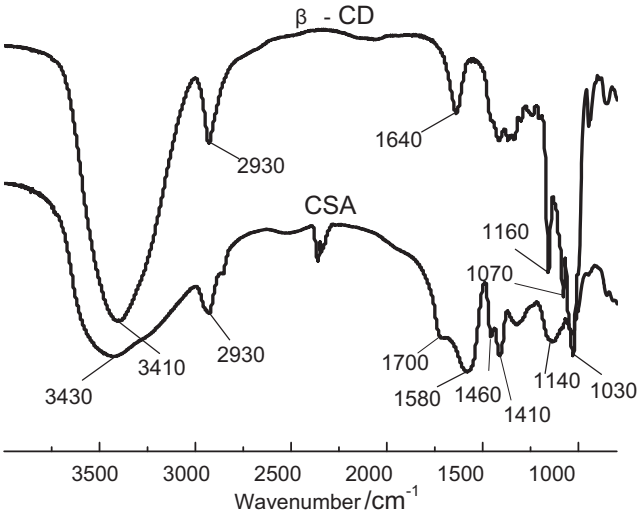

Fig. 2. FTIR spectra of β-CD and CSA.

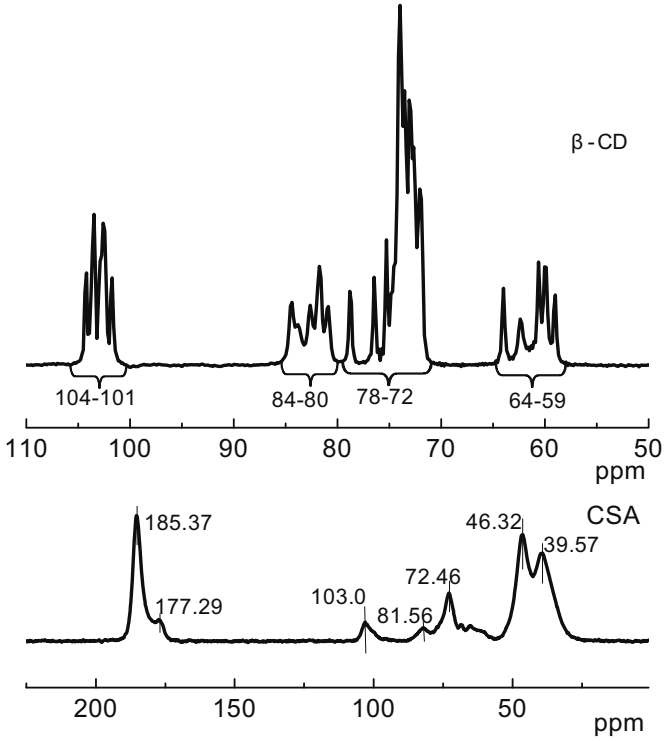

Fig. 3. Solid-state ^{13}C NMR spectra of β-CD and CSA.

groups are carbonyl groups from sodium polyacrylate salts and SA (Kuang, YuK, & Huh, 2011). The peaks at 1580 and 1460 cm^{-1} were from the asymmetric stretching vibrations of the carbonyl group of —COONa in the sodium polyacrylate salt, and a —C=O carbonyl bending vibration appeared at 1410 cm^{-1}. The results indicate that there are two main carbonyl groups in the polymer structure and this is evidence of the polymerization of β-CD, AA, and SA.

3.2.2. ^{13}C NMR analysis

The ^{13}C NMR spectrum of β-CD is shown in Fig. 3. The chemical shift peaks at 101–104 ppm are C1 signal peaks from the β-CD vertical glycosidic linkage. The chemical shifts at 80–84 ppm are the characteristic signals for C4. The chemical shifts at 72–78 ppm represent the cyclic carbons C2, C3, and C5, and these are not connected to the glycosidic bond. The separated peaks at 59–64 ppm are characteristic of the signal for C6 (Huang et al., 2012). In the ^{13}C NMR spectra of CSA, some chemical shift peaks overlapped but the chemical shifts at 72.46 ppm and 81.56 ppm, which are characteristic of C1, C2, C3, and C5 in β-CD still remained. In this study, the C2, C3, and C5 peaks overlapped to form a relatively broad peak (Lu, Yang, Zhou, & Lei, 2008), and a broad peak at around 60 ppm from C6 in β-CD appeared. The presence of these peaks indicated the introduction of β-CD into the product. The chemical shift peak at 185.37 ppm is a characteristic carbon atom peak for the carboxy group of AA. The peak at 177.24 ppm is from the carbon atom in the C=O of SA and the weak chemical shift peak at 103 ppm is from the C=C carbon atoms (Huang, Wu, Liu, Liu, & Zhang, 2013a). The above experimental results show that the polymerization of β-CD, AA, and SA had occurred.

3.2.3. SEM analysis

Fig. 4 shows SEM images of CSA dry resin (a) and CSA after water absorption (b) in different absorption media. As shown in Fig. 4(a), many pores of different sizes are present on the resin surface and the presence of these pores increases the resin surface area and improves the resin's exchange and absorption functions. After the absorption of distilled water by CSA (Fig. 4(b)), its internal structure expands to form an 8–20-μm-long polygonal three-dimensional grid structure. This three-dimensional grid structure of the CSA hydrogel not only improves the gel strength after water absorption but it also increases the water retention ability of CSA.

3.3. CSA water absorption in salt solutions

Fig. 5 shows the water absorbency of CSA in the presence of different cation concentrations in Cl^- and SO_4^{2-} salt solutions. As shown in Fig. 5, the CSA water absorbency trends were consistent for different salt concentrations, and a general decrease was found with an increase in the salt concentration. For the different cations in the Cl^- or SO_4^{2-} salt solutions the water absorbency of CSA decreased with an increase in cation valence at the same salt solution concentrations. At low ionic strength the CSA water absorbency in the monovalent cation salt solutions was much higher than that in the divalent or trivalent cation salt solutions. This increase in absorbency in the monovalent Na^+ and K^+ salt solutions was mainly the result of osmotic pressure in the CSA resin and the affinity between water and —COO^- in the network chain. The complexation constants between Na^+ and —COO^- and K^+ and —COO^- are small and, therefore, the water absorbency of CSA in Na^+ and K^+ salt solutions is relatively high. In divalent and trivalent metal cation salt solutions, metal cations chelated with —COO^- groups in the resin chain form crosslinking points, which decrease the CSA resin's network space and water absorbency. During the initial swelling period, the osmotic pressure is relatively large and the swelling effect is stronger than chelation thereby increasing the water absorbency. At the end of swelling, divalent and trivalent metal ions are easily chelated with the resin chains. The osmotic pressure decreases and the chelation effect are greater than the swelling effect resulting in a decrease in absorbency. The complex stability constants of the divalent and trivalent metal cations with —COO^- decrease as follows: $Fe^{3+} > Ca^{2+} > Mg^{2+}$. The ionic radius of Na^+ is smaller than that of K^+ and, therefore, at the same ionic strength the water absorbency of CSA in Na^+ salts is greater than that in K^+ salts (Bao et al., 2011). As shown in Fig. 4, at solution concentrations of 0.005–0.1 mol/L the order of CSA water absorbency in chloride salts decreases as follows: $NaCl > KCl > MgCl_2 > CaCl_2 > FeCl_3$, and that in sulfate salts is: $Na_2SO_4 > K_2SO_4 > FeSO_4 > Al_2(SO_4)_3$. In solutions with low salt concentrations, the CSA water absorbency was found to be relatively high and the resin had relatively good salt resistance. The liquid absorption ability of CSA was much lower in solutions with

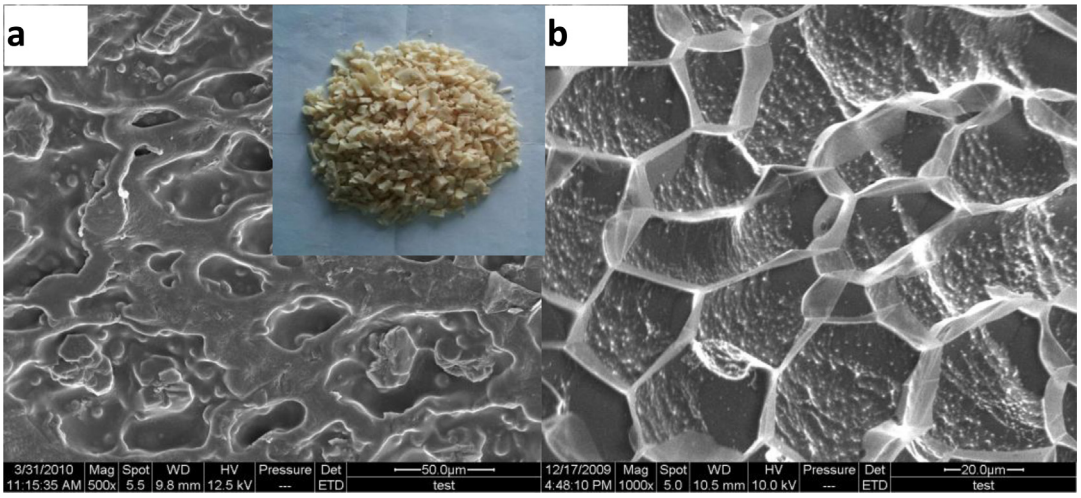

Fig. 4. SEM micrographs of (a) dry CSA and (b) in distilled water.

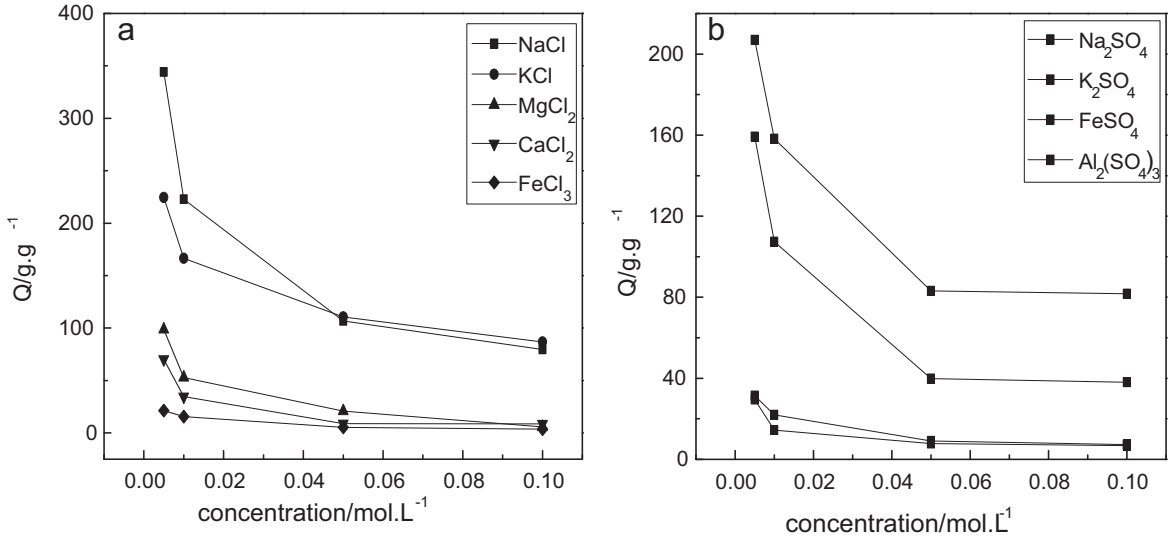

Fig. 5. Swelling curves of CSA in different salt solutions.

high salt concentrations. One reason is that the osmotic pressure of the CSA resin in a salt solution is less than that in distilled water. Another reason is that the ions in solution hinder the dissociation of the resin's ionic groups, which reduces the osmotic pressure of the resin and the electrostatic repulsion of the resin's molecular chains, and this leads to a relatively low water absorbency.

3.4. *Effects of pH on the absorbency of CSA*

The liquid absorption properties of CSA in buffer solutions at various pH values are shown in Fig. 6. The results show that the pH of the buffer solution has a significant influence on the absorbency of CSA. CSA is a pH-sensitive resin. When the pH is less than 2 the CSA resin almost does not swell. When the pH ranges is from 4 to 6, the absorbency of the CSA resin increases rapidly with increasing pH. When the solution pH ranges is from 6 to 14, the absorbency of CSA decreases sharply. The reason is that under strong acidic conditions, a large number of —COO^- groups in the CSA network chain are in the —COOH form resulting in minimal repulsion between the chains of the three-dimensional resin network. The resin absorbency is, therefore, very low at low pH values (Wang & Wang, 2010). As the pH increases, the —COO(H) groups of the resin chain are mainly present as —COO^- and the gel network chains repel one another.

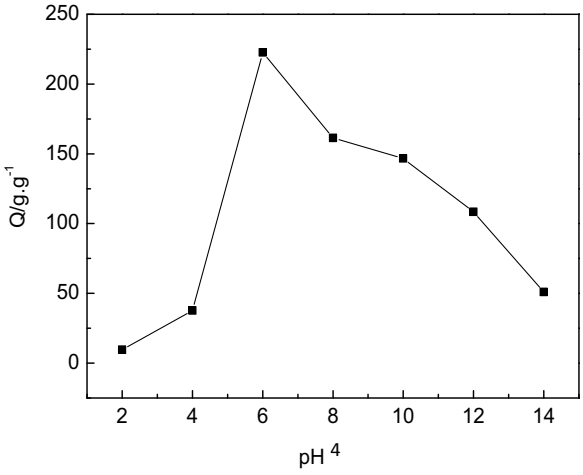

Fig. 6. Effect of CSA pH on water absorbency.

Because of the osmotic pressure difference and the hydrogen bonds between the ions, a large amount of water is enclosed within the network spaces after the expansion and the absorbency increases greatly. With a further increase in pH the osmotic pressure

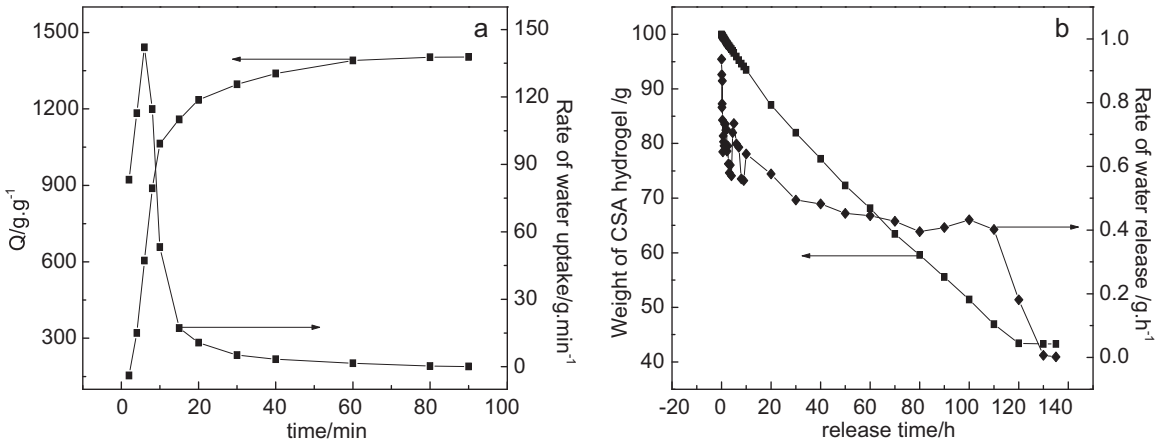

Fig. 7. Water absorption (a) and release (b) curves for CSA.

difference decreases and the retraction force of the network spaces increases, which limit water molecule access to the network spaces resulting in a slow decrease in absorbency.

3.5. Water absorption/retention by CSA

The effect of time on CSA water absorption/retention is shown in Fig. 7. Fig. 7(a) shows that for a water absorption time of $t < 6$ min the water absorption rate increased sharply and at an absorption time of $t = 6$ min the water absorption rate reached its maximum of 142 g/min. For a water absorption time from 0 to 15 min the CSA water absorbency increased sharply and the absorbency at equilibrium was more than 80%. At a water absorption time of 40 min, water absorption by CSA became saturated at a water absorbency of 1340 g/g. During the early period of water absorption, the ion concentration difference between the solutions within and outside the resin was relatively large, the osmotic pressure was high, the amount of water in the network was small, and the degree of network stretching was not significant resulting in the water absorption rate increasing rapidly. As the amount of water absorbed by the resin increased the CSA hydrogel elasticity rapidly increased and the osmotic pressure became small. Thus, the water absorption rate of the CSA resin decreased. When the water absorption and drainage effects were equal the absorption process was complete and its water absorption ability was saturated.

Fig. 7(b) shows a curve of the natural release of the water complexed within the CSA hydrogel with time. This figure shows that the weight and release rate of the CSA hydrogel increased with time. The water retention time of the CSA hydrogel was relatively long at 120 h. The mass and the water release rate of the CSA hydrogel after natural release over 120 h remained almost constant. This is because during swelling, the water molecules form hydrogen bonds with CSA and the hydrogen bonds allow water molecules to attach to the polymer chains of CSA. The energy of water release from the polymer network structure is higher than that from the water phase. In addition, during the natural release of water molecules from the CSA hydrogel, a film is formed on the CSA hydrogel surface and this reduces the water molecule release rate. These results show that CSA has excellent water retention properties.

3.6. Biodegradation of CSA

The degradation efficiency of CSA gel and PAA in *Penicillium*, *Aspergillus niger*, and *Lentinula edodes* were obtained in this study (Fig. 8). As shown in Fig. 8, the CSA gel degradation efficiency increased rapidly with time in *L. edodes*. The degradation efficiency of CSA gel reached 73.2% after 3 days, and 85.3% after 12 days. Also,

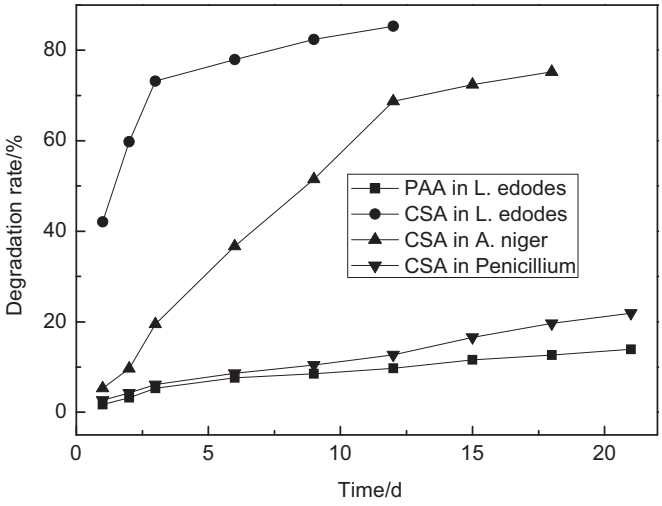

Fig. 8. Mycete degradation of CSA and PAA.

in 6 days, the block samples turned into fluid. The degradation efficiency increased slowly in *Penicillium* with only 6.11% of the CSA gel was degraded after 3 days and 21.49% after 21 days. In *A. niger*, the degradation efficiency of CSA gel increased rapidly with time. After 3 days, the degradation efficiency was 15.9%, and reached 68.7% after 21days. The results shown that *L. edodes* degrades better than the other mycetes, and that the CSA gel is biodegradable and it has an excellent degradation efficiency in *L. edodes*. However, the degradation efficiency of poly acrylic acid (PAA) resin in *L. edodes* was just 7.6% after 6 days, and 9.7% after 12 days, with degradation efficiency reaching a maximum of 13.9% after 21 days. The degradation of CSA gel was observed to be very faster with *L. edodes* than PAA resin. As a result, the CSA is a novel eco-friendly and biodegradable material.

4. Conclusions

A superabsorbent polymer, CSA, with a three-dimensional network structure was self-assembled using inverse suspension graft copolymerization. This resin is biodegradable and has a good three-dimensional network structure because of the introduction of β-CD. The CSA water retention time was relatively long and the water in the CSA hydrogel was released slowly over 120 h. The CSA gel has excellent water absorption and water retention properties. The CSA also has good salt resistance toward chloride and sulfate

salts and it shows promise for future agricultural applications as a water retention agent.

Acknowledgment

This work was supported by the Fundamental Research Funds for the Central Universities (No. 2572014DB01).

References

Achtenhagen, J., & Kreuzi, R. (2011). Laboratory tests on the impact of superabsorbent polymers on transformation and sorption of xenobiotics in soil taking ^{14}C-imazalil as an example science of the total environment. *Science of the Total Environment*, *409*(24), 5454–5458.

Badruddoza, A. Z. M., Tay, A. S. H., Tan, P. Y., Hidajat, K., & Uddin, M. S. (2011). Carboxymethyl-β-cyclodextrin conjugated magnetic nanoparticles as nano-adsorbents for removal of copper ions: Synthesis and adsorption studies. *Journal of Hazardous Materials*, *185*(2–3), 1177–1186.

Bao, Y., Ma, J. Z., & Li, N. (2011). Synthesis and swelling behaviors of sodium carboxymethyl cellulose-*g*-poly (AA-*co*-AM-*co*-AMPS)/MMT superabsorbent hydrogel. *Carbohydrate Polymers*, *84*(1), 76–82.

Blanco-Fernandez, B., Lopez-Viota, M., Concheiro, A., & Alvarez-Lorenzo, C. (2011). Synergistic performance of cyclodextrin–agar hydrogels for ciprofloxacin delivery and antimicrobial effect. *Carbohydrate Polymers*, *85*(4), 765–774.

Barsbay, M., & Güven, O. (2013). RAFT mediated grafting of poly(acrylic acid) (PAA) from polyethylene/polypropylene (PE/PP) nonwoven fabric via preirradiation. *Polymers*, *54*(18), 4838–4848.

Huang, Z. H., Liu, S. X., Zhang, B., Xu, L. L., & Hu, X. F. (2012). Equilibrium and kinetics studies on the adsorption of Cu(II) from the aqueous phase using a β-cyclodextrin-based adsorbent. *Carbohydrate Polymers*, *88*, 609–617.

Huang, Z. H., Wu, Q. L., Liu, S. X., Liu, T., & Zhang, B. (2013). A novel biodegradable β-cyclodextrin-based hydrogel for the removal of heavy metal ions. *Carbohydrate Polymers*, *97*(2), 496–502.

Huang, Z. H., Liu, S. X., Fang, G. Z., & Zhang, B. (2013). Synthesis and swelling properties of β-cyclodextrin-based superabsorbent resin with network structure. *Carbohydrate Polymers*, *92*(2), 2314–2320.

Kabiri, K., Omidian, H., Zohuriaan-Mehr, M. J., & Doroudiani, S. (2011). Superabsorbent hydrogel composites and nanocomposites: A review. *Polymer Composites*, *32*(2), 277–289.

Kuang, J., YuK, K. Y., & Huh, K. M. (2011). Polysaccharide-based superporous hydrogels with fast swelling and superabsorbent properties. *Carbohydrate Polymers*, *83*, 284–290.

Li, P., Kim, N. H., & Lee, J. H. (2009). Swelling behavior of polyacrylamide/laponite clay nanocomposite hydrogels: pH-sensitive property. *Composites Part B: Engineering*, *40*(4), 275–283.

Lu, D. D., Yang, L. Q., Zhou, T. H., & Lei, Z. Q. (2008). Synthesis, characterization and properties of biodegradable polylactic acid-β-cyclodextrin cross-linked copolymer microgels. *European Polymer Journal*, *44*, 2140–2145.

Peng, G., Xu, S. M., Peng, Y., Wang, J. D., & Zheng, L. C. (2008). A new amphoteric superabsorbent hydrogel based on sodium starch sulfate. *Bioresource Technology*, *99*, 444–447.

Pourjava, A., & Amini-Fazl, M. S. (2007). Optimized synthesis of carrageenan graft-poly(sodium acrylate) super-absorbent hydroxyl using the Taguchi method and investigation of its metal ion absorption. *Polymer International*, *56*, 283–289.

Ma, Z. H., Li, Q., Yue, Q. Y., Gao, B. Y., Xu, X., & Zhong, Q. Q. (2011). Synthesis and characterization of a novel super-absorbent based on wheat straw. *Bioresource Technology*, *102*, 2853–2858.

Misiuk, W., & Zalewska, M. (2009). Investigation of inclusion complex of trazodone hydrochloride with hydroxypropyl-β-cyclodextrin. *Carbohydrate Polymers*, *77*(3), 482–488.

Murthy, S. N., Madhav, B., Kumar, A. V., Rao, K. R., & Nageswar, Y. V. D. (2009). Multicomponent approach towards the synthesis of substituted pyrroles under supramolecular catalysis using β-cyclodextrin as a catalyst in water under neutral conditions. *Helvetica Chimica Acta*, *92*(10), 2118–2124.

Shao, D., Sheng, G., Chen, C., Wang, X., & Nagatsu, M. (2010). Removal of polychlorinated biphenyls from aqueous solutions using β-cyclodextrin grafted multiwalled carbon nanotubes. *Chemosphere*, *79*(7), 679–685.

Srinivasachari, S., & Reineke, T. M. (2009). Versatile supramolecular pDNA vehicles via "click polymerization" of β-cyclodextrin with oligoethyleneamines. *Biomaterials*, *30*(5), 928–938.

Wang, W. B., & Wang, A. Q. (2010). Synthesis and swelling properties of pH-sensitive semi-IPN superabsorbent hydrogels based on sodium alginate-*g*-poly(sodium acrylate) and polyvinylpyrrolidone. *Carbohydrate Polymers*, *80*, 1028–1036.

Xu, J., Li, X., & Sun, F. (2010). Cyclodextrin-containing hydrogels for contact lenses as a platform for drug incorporation and release. *Acta Biomaterialia*, *6*, 486–493.

Yallapu, M. M., Jaggi, M., & Chauhan, S. C. (2010). β-Cyclodextrin-curcumin self-assembly enhances curcumin delivery in prostate cancer cells. *Colloids and Surfaces B: Biointerfaces*, *79*(1), 113–125.

Yang, J. S., Xie, Y. J., & He, W. (2011). Research progress on chemical modification of alginate: A review. *Carbohydrate Polymers*, *84*(1), 33–39.

Lv, Y. X. (2011). Status and trend of domestic and overseas markets for acrylic industry. *Fine and Specialty Chemicals*, *19*(6), 5–10.

Zhang, W., Qin, L., He, X. W., Li, W. Y., & Zhang, Y. K. (2009). Novel surface modified molecularly imprinted polymer using acryloyl-β-cyclodextrin and acrylamide as monomers for selective recognition of lysozyme in aqueous solution,. *Journal of Chromatography A*, *1216*(21), 4560–4567.

Zou, W., Yu, L., Liu, X. X., Chen, L., Zhang, X. Q., & Qiao, D. (2012). Effects of amylose/amylopectin ratio on starch-based superabsorbent polymers. *Carbohydrate Polymers*, *87*(2), 1583–1588.